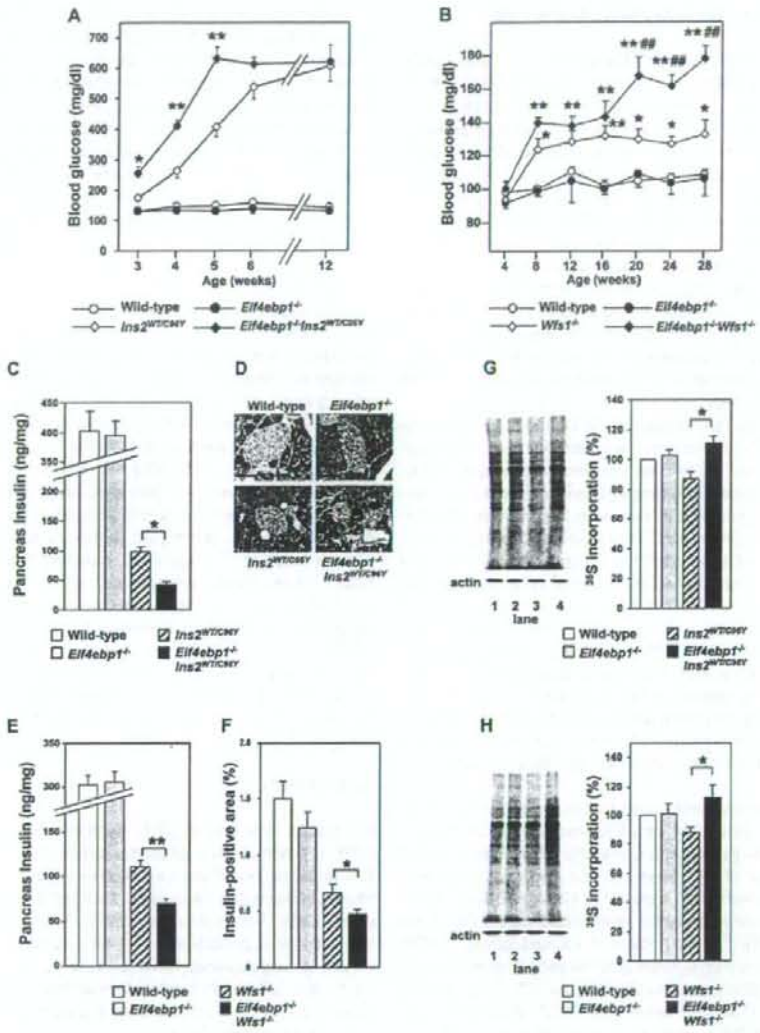

Figure 4. β Cell Loss Is Exacerbated by 4E-BP1 Deficiency in Mouse Diabetes Models

(A) Fed blood glucose levels of wild-type (n = 6), *Eif4ebp1*$^{-/-}$ (n = 5), *Ins2*$^{WT/C96Y}$ (n = 9), and *Eif4ebp1*$^{-/-}$ *Ins2*$^{WT/C96Y}$ (n = 11) mice. Data from three cohorts are combined. *p < 0.05, **p < 0.01 versus *Ins2*$^{WT/C96Y}$ mice.

(B) Fed blood glucose levels of wild-type (n = 12), *Eif4ebp1*$^{-/-}$ (n = 8), *Wfs1*$^{-/-}$ (n = 15), and *Eif4ebp1*$^{-/-}$ *Wfs1*$^{-/-}$ (n = 10) mice. Data from three cohorts are combined. *p < 0.05, **p < 0.01 versus wild-type mice; ##p < 0.01 versus *Wfs1*$^{-/-}$ mice.

(C) Pancreatic insulin content of mice of the indicated genotypes at 5 weeks of age. n = 3 for each genotype. *p < 0.05.

(D) Hematoxylin and eosin staining of sections showing representative islets from mice of the indicated genotypes at 5 weeks of age. Scale bars = 50 μm.

(E) Pancreatic insulin content of wild-type (n = 8), *Eif4ebp1*$^{-/-}$ (n = 4), *Wfs1*$^{-/-}$ (n = 15), and *Eif4ebp1*$^{-/-}$ *Wfs1*$^{-/-}$ (n = 12) mice at 27–30 weeks of age. **p < 0.01.

(F) Insulin-positive area in pancreatic sections of wild-type (n = 3), *Eif4ebp1*$^{-/-}$ (n = 3), *Wfs1*$^{-/-}$ (n = 4), and *Eif4ebp1*$^{-/-}$ *Wfs1*$^{-/-}$ (n = 5) mice at 27–30 weeks of age. *p < 0.05.

(G) [^{35}S]methionine/cysteine incorporation in islets of the indicated genotypes at 5–6 weeks of age. Ten percent of the lysates were also probed with an anti-actin antibody. A representative autoradiogram is shown in the left panel. Lane 1, wild-type; lane 2, *Eif4ebp1*$^{-/-}$; lane 3, *Ins2*$^{WT/C96Y}$; lane 4, *Eif4ebp1*$^{-/-}$ *Ins2*$^{WT/C96Y}$. Data from four experiments are summarized in the right panel. *p < 0.05.

ATF4, the primary inducer of *Eif4ebp1* under ER stress, is activated by translational suppression by eIF2α phosphorylation during the acute phase. We found that 4E-BP1 protein is stable with a half-life of approximately 20 hr (Figure S6). Thus, 4E-BP1 protein seems to continue to be expressed abundantly during the later stages of the UPR. This is consistent with the recent observation that several prosurvival proteins involved in the UPR are stable, while proapoptotic proteins are not (Rutkowski et al., 2006). We found that global protein synthesis was higher in 4E-BP1-deficient β cells than in wild-type cells under ER stress conditions. In particular, expression of CHOP was augmented in 4E-BP1 deficiency. Enhanced CHOP expression in 4E-BP1-deficient cells suggests that a reduction in eIF4E availability due to 4E-BP1 induction suppresses CHOP translation during ER stress in wild-type cells, possibly accounting for one of the mechanisms by which 4E-BP1 plays a role in adaptation to ER stress. Important roles of translational control via eIF4E availability have also been suggested in prolonged hypoxia (Koritzinsky et al., 2006). However, the signaling mechanisms for translational control are different: ER stress increases 4E-BP1 protein levels via ATF4 in β cells, while hypoxia enhances 4E-BP1 activity via dephosphorylation and also causes eIF4E nuclear localization in HeLa cells.

The present results also suggest that variations in genes regulating eIF4E availability and/or eIF4F formation may have an impact on susceptibility to diabetes. In this context, a recent report demonstrating that a gene encoding eIF4A2, a component of eIF4F, is possibly linked to type 2 diabetes in French families (Cheyssac et al., 2006) is of great interest. Furthermore, our findings raise the possibility that 4E-BP1 may be a potential target for diabetes mellitus treatment.

EXPERIMENTAL PROCEDURES

Animal Experiments

All animal experiments were approved by the Tohoku University Institutional Animal Care and Use Committee. *Wfs1*$^{-/-}$ mice were backcrossed to a 129S6 (Taconic) background for six generations. *Ins2*$^{WT/C96Y}$ mice (Charles River Laboratories) were backcrossed to a 129S6 background for five generations. *Eif4ebp1*$^{-/-}$ mice were maintained on a 129S6 background. Only male mice were used. For the in vivo studies shown in Figures 4A, 4C, and 4D, littermates from crosses of male *Ins2*$^{WT/C96Y}$ *Eif4ebp1*$^{+/-}$ and female *Ins2*$^{WT/WT}$ *Eif4ebp1*$^{+/-}$ mice were used. For Figures 4B, 4E, and 4F, littermates from intercrosses of *Eif4ebp1*$^{+/-}$ *Wfs1*$^{+/+}$ mice and littermates from intercrosses of *Eif4ebp1*$^{+/-}$ *Wfs1*$^{-/-}$ mice were used. For isolated islet experiments (Figures 4G and 4H), age-matched nonlittermate mice were used. To induce ER stress in vivo, mice were given a 0.5 μg/g body weight intraperitoneal injection of tunicamycin. After 96 hr, kidneys and livers were removed. Tissue sample processing, immunostaining of pancreatic sections, and determination of β cell area and pancreatic insulin content were performed as described previously (Ishihara et al., 2004).

Cell Culture and Cell Viability Assay

Pancreatic tumors in *Eif4ebp1*$^{-/-}$:SV40Tag mice on a mixed background were excised, yielding MIN6*Eif4ebp1*$^{-/-}$cells, which were used at 5–10 passages in this study. MIN6 cells were cultured in DMEM supplemented with 15% FCS. *Atf4*$^{-/-}$ MEFs were cultured in DMEM supplemented with a nonessential amino acid mixture and 10% FCS. Cells seeded in 24-well plates 2 days previously were treated with thapsigargin or tunicamycin and used for western blotting or cell viability assay. Cell viability was determined with a cell proliferation assay kit (Promega). Construction of adenoviruses and infection of MIN6 cells were performed as described previously (Ishihara et al., 2004).

Northern and Western Blotting and Cap-Binding Affinity Assay

Total RNA extracted using ISOGEN (Nippon Gene) was probed with ^{32}P-labeled cDNAs. Tissue homogenates and cell lysates were subjected to SDS-PAGE and probed with primary antibodies against 4E-BP1, 4E-BP2, eIF4E, eIF4G, cleaved caspase-3 (Cell Signaling), ATF4, CHOP (Santa Cruz), and actin (Sigma). Cell lysates were incubated with 7-methyl-GTP (^{7}mGTP)-Sepharose (Amersham) overnight at 4°C. The ^{7}mGTP-Sepharose was then pelleted and boiled. Experiments were performed at least three times. Band intensity was quantified using Scion Image software.

Metabolic Labeling

Due to the low islet yields from *Ins2*$^{WT/C96Y}$, *Ins2*$^{WT/C96Y}$ *Eif4ebp1*$^{-/-}$, *Wfs1*$^{-/-}$, and *Eif4ebp1*$^{-/-}$ *Wfs1*$^{-/-}$ mice, islets with these genotypes were pooled from two or three mice. Fifty to eighty islets were cultured for 3 days in RPMI supplemented with 10% FCS. Islets washed with methionine/cysteine-free RPMI containing 10% dialyzed FCS were labeled with a protein labeling mix (PerkinElmer) (1.0 MBq/tube) for 15 min and then resolved in sample buffer (1.0 μl/islet for wild-type and *Eif4ebp1*$^{-/-}$ islets and 0.75 μl/islet for other genotypes). The level of protein synthesis was quantified from autoradiograms. For measurement of *Chop* translation, 4 × 10^6 cells treated with thapsigargin for 12 hr were washed with methionine/cysteine-free DMEM containing 15% dialyzed FCS and labeled with [^{35}S]methionine/cysteine (20 MBq/bottle) for 2 hr. Cells were then resolved in lysis buffer (50 mM Tris [pH 7.5], 150 mM NaCl, 2 mM $MgCl_2$, 0.1% Triton X-100, and protease inhibitors [Roche]). Lysates were precleared with Protein A Sepharose Fast Flow (Amersham) and incubated with anti-CHOP antibody (R-20, Santa Cruz) overnight.

Firefly Luciferase Reporter Assay

Oligonucleotides containing ATF4 binding sites were annealed and subcloned into the pGL3-Promoter vector (BamHI-SalI, Promega). MIN6 cells were transfected with luciferase reporters using Lipofectamine (Invitrogen). Luciferase activity was assayed with a dual-luciferase system (Promega) using a luminometer (Berthold).

Chromatin Immunoprecipitation Assay

Proteins bound to DNA were crosslinked with 1% formaldehyde at 4°C for 20 min. After sonication, the protein-DNA complexes were immunoprecipitated using an anti-ATF4 antibody (C-20, Santa Cruz). After reversal of the crosslinks at 65°C for 6 hr, DNA was purified on a DNA purification column (QIAGEN). PCR was performed with the primers 5′-GATGAGGAAGAGGAAGCTGAGT TG-3′ and 5′-AGTTGTAAGAGGAGTAGTTGGGGG-3′.

Statistical Analysis

Data are presented as means ± SEM. Differences between groups were assessed by Student's t test. $p < 0.05$ was considered significant.

SUPPLEMENTAL DATA

Supplemental Data include six figures and Supplemental References and can be found with this article online at http://www.cellmetabolism.org/cgi/content/full/7/3/269/DC1/.

ACKNOWLEDGMENTS

We thank J. Alam (Alton Ochsner Medical Foundation) and D. Ron (New York University) for their generous gifts of DN-ATF4 cDNA and *Atf4*$^{-/-}$ MEFs, respectively. We are also grateful to K. Igarashi (Tohoku University) for advice on ChIP analysis and to Y. Nagura and K. Tanaka for their expert technical assistance. This work was supported by Grants-in-Aid for Scientific Research

(H) [^{35}S]methionine/cysteine labeling as in (G) in islets of the indicated genotypes at 6–8 weeks of age. Lane 1, wild-type; lane 2, *Eif4ebp1*$^{-/-}$; lane 3, *Wfs1*$^{-/-}$; lane 4, *Eif4ebp1*$^{-/-}$ *Wfs1*$^{-/-}$. Data from three experiments are summarized in the right panel. *$p < 0.05$.
Error bars represent SEM.

(19590300 to H.I. and 19209034 to Y.O.) from the Ministry of Education, Culture, Sports, Science and Technology of Japan.

Received: July 10, 2007
Revised: December 2, 2007
Accepted: January 30, 2008
Published: March 4, 2008

REFERENCES

Butler, A.E., Janson, J., Bonner-Weir, S., Ritzel, R., Rizza, R.A., and Butler, P.C. (2003). β-cell deficit and increased beta-cell apoptosis in humans with type 2 diabetes. Diabetes *52*, 102–110.

Cheyssac, C., Dina, C., Lepretre, F., Vasseur-Delannoy, V., Dechaume, A., Lobbens, S., Balkau, B., Ruiz, J., Charpentier, G., Pattou, F., et al. (2006). EIF4A2 is a positional candidate gene at the 3q27 locus linked to type 2 diabetes in French families. Diabetes *55*, 1171–1176.

Clemens, M.J. (2001). Translational regulation in cell stress and apoptosis. Roles of the eIF4E binding proteins. J. Cell. Mol. Med. *5*, 221–239.

Delepine, M., Nicolino, M., Barrett, T., Golamaully, M., Lathrop, G.M., and Julier, C. (2000). EIF2AK3, encoding translation initiation factor 2-alpha kinase 3, is mutated in patients with Wolcott-Rallison syndrome. Nat. Genet. *25*, 406–409.

Harding, H.P., Novoa, I., Zhang, Y., Zeng, H., Wek, R., Schapira, M., and Ron, D. (2000). Regulated translation initiation controls stress-induced gene expression in mammalian cells. Mol. Cell *6*, 1099–1108.

Harding, H.P., Zeng, H., Zhang, Y., Jungries, R., Chung, P., Plesken, H., Sabatini, D.D., and Ron, D. (2001). Diabetes mellitus and exocrine pancreatic dysfunction in perk−/− mice reveals a role for translational control in secretory cell survival. Mol. Cell *7*, 1153–1163.

Harding, H.P., Zhang, Y., Zeng, H., Novoa, I., Lu, P.D., Calfon, M., Sadri, N., Yun, C., Popko, B., Paules, R., et al. (2003). An integrated stress response regulates amino acid metabolism and resistance to oxidative stress. Mol. Cell *11*, 619–633.

He, C.H., Gong, P., Hu, B., Stewart, D., Choi, M.E., Choi, A.M., and Alam, J. (2001). Identification of activating transcription factor 4 (ATF4) as an Nrf2-interacting protein. Implication for heme oxygenase-1 gene regulation. J. Biol. Chem. *276*, 20858–20865.

Holcik, M., and Sonenberg, N. (2005). Translational control in stress and apoptosis. Nat. Rev. Mol. Cell Biol. *6*, 318–327.

Ibrahimo, S., Holmes, L.E., and Ashe, M.P. (2006). Regulation of translation initiation by the yeast eIF4E binding proteins is required for the pseudohyphal response. Yeast *23*, 1075–1088.

Inoue, H., Tanizawa, Y., Wasson, J., Behn, P., Kalidas, K., Bernal-Mizrachi, E., Mueckler, M., Marshall, H., Donis-Keller, H., Crock, P., et al. (1998). A gene encoding a transmembrane protein is mutated in patients with diabetes mellitus and optic atrophy (Wolfram syndrome). Nat. Genet. *20*, 143–148.

Ishihara, H., Takeda, S., Tamura, A., Takahashi, R., Yamaguchi, S., Takei, D., Yamada, T., Inoue, H., Soga, H., Katagiri, H., et al. (2004). Disruption of the WFS1 gene in mice causes progressive beta-cell loss and impaired stimulus-secretion coupling in insulin secretion. Hum. Mol. Genet. *13*, 1159–1170.

Koritzinsky, M., Magagnin, M.G., van den Beucken, T., Seigneuric, R., Savelkouls, K., Dostie, J., Pyronnet, S., Kaufman, R.J., Weppler, S.A., Voncken, J.W., et al. (2006). Gene expression during acute and prolonged hypoxia is regulated by distinct mechanisms of translational control. EMBO J. *25*, 1114–1125.

Laybutt, D.R., Preston, A.M., Akerfeldt, M.C., Kench, J.G., Busch, A.K., Biankin, A.V., and Biden, T.J. (2007). Endoplasmic reticulum stress contributes to beta cell apoptosis in type 2 diabetes. Diabetologia *50*, 752–763.

Miyazaki, J., Araki, K., Yamato, E., Ikegami, H., Asano, T., Shibasaki, Y., Oka, Y., and Yamamura, K. (1990). Establishment of a pancreatic beta cell line that retains glucose-inducible insulin secretion: special reference to expression of glucose transporter isoforms. Endocrinology *127*, 126–132.

Novoa, I., and Carrasco, L. (1999). Cleavage of eukaryotic translation initiation factor 4G by exogenously added hybrid proteins containing poliovirus 2Apro in HeLa cells: effects on gene expression. Mol. Cell. Biol. *19*, 2445–2454.

Novoa, I., Zeng, H., Harding, H.P., and Ron, D. (2001). Feedback inhibition of the unfolded protein response by GADD34-mediated dephosphorylation of eIF2α. J. Cell Biol. *153*, 1011–1022.

Pirot, P., Naamane, N., Libert, F., Magnusson, N.E., Orntoft, T.F., Cardozo, A.K., and Eizirik, D.L. (2007). Global profiling of genes modified by endoplasmic reticulum stress in pancreatic beta cells reveals the early degradation of insulin mRNAs. Diabetologia *50*, 1006–1014.

Riggs, A.C., Bernal-Mizrachi, E., Ohsugi, M., Wasson, J., Fatrai, S., Welling, C., Murray, J., Schmidt, R.E., Herrera, P.L., and Permutt, M.A. (2005). Mice conditionally lacking the Wolfram gene in pancreatic islet beta cells exhibit diabetes as a result of enhanced endoplasmic reticulum stress and apoptosis. Diabetologia *48*, 2313–2321.

Rutkowski, D.T., Arnold, S.M., Miller, C.N., Wu, J., Li, J., Gunnison, K.M., Mori, K., Sadighi Akha, A.A., Raden, D., and Kaufman, R.J. (2006). Adaptation to ER stress is mediated by differential stabilities of pro-survival and pro-apoptotic mRNAs and proteins. PLoS Biol. *4*, e374.

Scheuner, D., Mierde, D.V., Song, B., Flamez, D., Creemers, J.W., Tsukamoto, K., Ribick, M., Schuit, F.C., and Kaufman, R.J. (2005). Control of mRNA translation preserves endoplasmic reticulum function in β cells and maintains glucose homeostasis. Nat. Med. *11*, 757–764.

Schroder, M., and Kaufman, R.J. (2005). The mammalian unfolded protein response. Annu. Rev. Biochem. *74*, 739–789.

Strom, T.M., Hortnagel, K., Hofmann, S., Gekeler, F., Scharfe, C., Rabl, W., Gerbitz, K.D., and Meitinger, T. (1998). Diabetes insipidus, diabetes mellitus, optic atrophy and deafness (DIDMOAD) caused by mutations in a novel gene (wolframin) coding for a predicted transmembrane protein. Hum. Mol. Genet. *7*, 2021–2028.

Teleman, A.A., Chen, Y.W., and Cohen, S.M. (2005). 4E-BP functions as a metabolic brake used under stress conditions but not during normal growth. Genes Dev. *19*, 1844–1848.

Tettweiler, G., Miron, M., Jenkins, M., Sonenberg, N., and Lasko, P.F. (2005). Starvation and oxidative stress resistance in Drosophila are mediated through the eIF4E-binding protein, d4E-BP. Genes Dev. *19*, 1840–1843.

Tsukiyama-Kohara, K., Poulin, F., Kohara, M., DeMaria, C.T., Cheng, A., Wu, Z., Gingras, A.C., Katsume, A., Elchebly, M., Spiegelman, B.M., et al. (2001). Adipose tissue reduction in mice lacking the translational inhibitor 4E-BP1. Nat. Med. *7*, 1128–1132.

Wang, J., Takeuchi, T., Tanaka, S., Kubo, S.K., Kayo, T., Lu, D., Takata, K., Koizumi, A., and Izumi, T. (1999). A mutation in the insulin 2 gene induces diabetes with severe pancreatic β-cell dysfunction in the Mody mouse. J. Clin. Invest. *103*, 27–37.

Zhang, P., McGrath, B., Li, S., Frank, A., Zambito, F., Reinert, J., Gannon, M., Ma, K., McNaughton, K., and Cavener, D.R. (2002). The PERK eukaryotic initiation factor 2α kinase is required for the development of the skeletal system, postnatal growth, and the function and viability of the pancreas. Mol. Cell. Biol. *22*, 3864–3874.

Cell Metabolism, Volume 7

Supplemental Data

Short Article

ATF4-Mediated Induction of 4E-BP1 Contributes to Pancreatic β Cell Survival under Endoplasmic Reticulum Stress

Suguru Yamaguchi, Hisamitsu Ishihara, Takahiro Yamada, Akira Tamura, Masahiro Usui, Ryu Tominaga, Yuichiro Munakata, Chihiro Satake, Hideki Katagiri, Fumi Tashiro, Hiroyuki Aburatani, Kyoko Tsukiyama-Kohara, Jun-ichi Miyazaki, Nahum Sonenberg, and Yoshitomo Oka

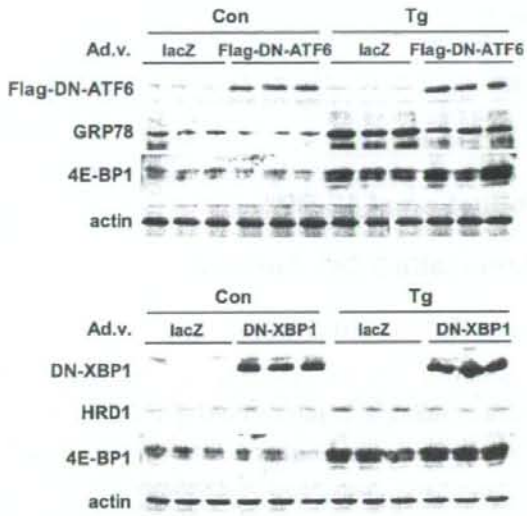

Figure S1. Effects of DN-ATF or DN-XBP1 Expression on 4E-BP1 Induction

Upper panel: no suppression of thapsigargin-triggered 4E-BP1 induction with expression of the Flag-tagged dominant-negative (DN) ATF6 (Flag-DN-ATF6: ATF6(171-373) lacking the activation domain (Yoshida et al., 2000)). MIN6 cells infected with an adenovirus expressing either lacZ or the Flag-DN-ATF6 were treated with vehicle (0.05% DMSO) control (Con) or thapsigargin (Tg, 0.5 μM) for 12 hr. Cell lysates were analyzed for expressions of Flag-DN-ATF6, GRP78 (ATF6-target), 4E-BP1 and actin (loading control).

Lower panel: no suppression of Tg-triggered 4E-BP1 induction with expression of the DN-XBP1 (XBP1(1-188) lacking the activation domain (Lee et al., 2003)). MIN6 cells infected with an adenovirus expressing either lacZ or the DN-XBP1 were treated with vehicle control (Con) or Tg for 12 hr. Cell lysates were analyzed for expressions of DN-XBP1, HRD1 (XBP1-target), 4E-BP1 and actin (loading control).

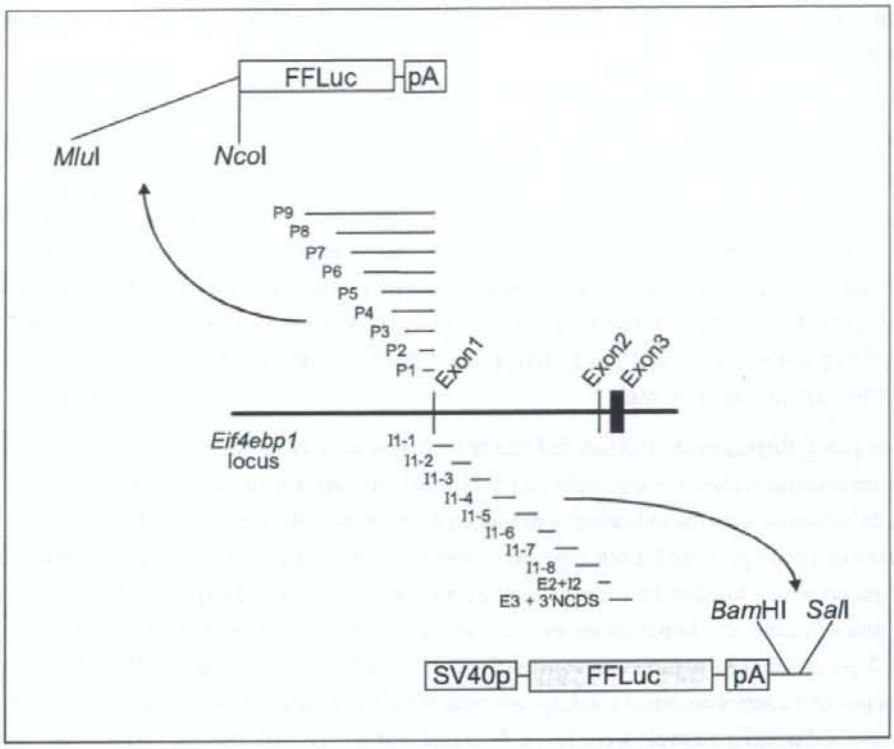
FFLuc
pA
MluI
NcoI
P9
P8
P7
P6
P5
P4
P3
P2
P1
Exon1
Exon2
Exon3
Eif4ebp1
locus
I1-1
I1-2
I1-3
I1-4
I1-5
I1-6
I1-7
I1-8
E2+I2
E3 + 3'NCDS
BamHI
SalI
SV40p
FFLuc
pA

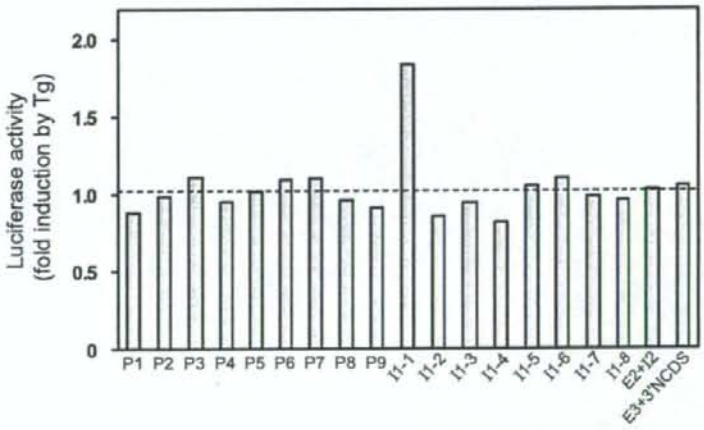
Luciferase activity
(fold induction by Tg)
2.0
1.5
1.0
0.5
0
P1
P2
P3
P4
P5
P6
P7
P8
P9
I1-1
I1-2
I1-3
I1-4
I1-5
I1-6
I1-7
I1-8
E2+I2
E3+3'NCDS

Figure S2. Search for Mouse *Eif4ebp1* Gene Segments Conferring Tg Responsiveness to Luciferase Reporter Constructs

Upper panel: reporter constructs used for luciferase activity measurements are presented. PCR-amplified *Eif4ebp1* promoter segments were cloned into the pGL3-basic construct (Promega). P1, -1 to –260 (A in the initial ATG codon is determined as +1); P2, -1 to -1,129; P3, -1 to -2,216; P4, -1 to -3,182; P5, -1 to –4,027; P6, -1 to -4,791; P7, -1 to –6,537; P8, -1 to -7,978; P9, -1 to -9,968. PCR-amplified *Eif4ebp1* segments spanning from exon 1 to the 3' non-coding sequence (3'NCDS) were cloned into the pGL3-promoter construct (Promega). I1-1, +1 to 1,821; I1-2, 1,821 to 3,409; I1-3, 3,409 to 5,198; I1-4, 5,198 to 6,957; I1-5, 6,957 to 8,752; I1-6, 8,752 to 9,977; I1-7, 9,977 to 11,804; I1-8, 11,804 to 12,949; E2+I2, 12,921 to 14,703; E3+3'NCDS, 14,704 to 16,260.

Lower panel: thapsigargin (Tg)-induced firefly luciferase activity in MIN6 cells transfected with reporter constructs shown in the upper panel. Firefly luciferase activity was normalized to Renilla luciferase activity and ratios of normalized activities in the presence to those in the absence of Tg are presented. Each experiment was performed employing 1 or 2 constructs and all data are presented together in one panel. Values are the means of 1 to 3 experiments, each performed in triplicate. Experiments were always conducted with a negative control construct (pGL3-promoter: a *SV40* promoter construct with no insertion between the *Bam*HI and *Sal*I sites) and a positive control construct (pGL3-basic with the *Chop* promoter). Fold inductions of the negative and positive controls were 1.03 ± 0.09 and 3.04 ± 0.11-fold (n = 25), respectively. Data obtained with the negative control are shown as a dashed line.

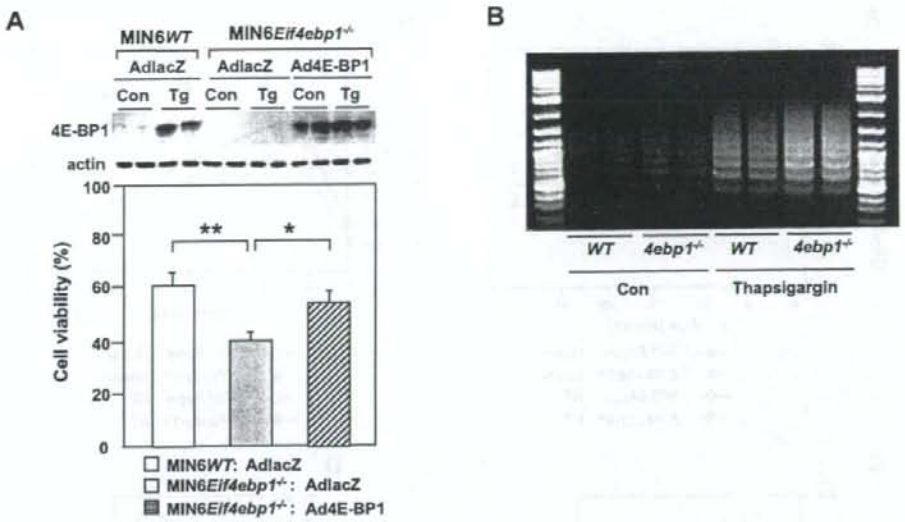

Figure S3. Higher Sensitivity of 4E-BP1-Deficient MIN6 Cells and Islets to ER Stress

(A) Reduced viability of MIN6*Eif4ebp1*$^{-/-}$ cells treated with 0.5 μM thapsigargin (Tg) was restored by re-expression of 4E-BP1. Data from MIN6*WT* cells treated with vehicle (0.05% DMSO) were taken as 100%. Error bars show SEM. n = 4; *$p < 0.05$, **$p < 0.01$. Adenovirus-mediated re-expression of 4E-BP1 is shown in the upper panel. Con, vehicle-treated cells.

(B) Increased apoptotic DNA ladder formation in isolated islets from *Eif4ebp1*$^{-/-}$ mice. Islets isolated from mice of each genotype at 12 weeks of age were incubated in RPMI medium for 3 days and DNA fragmentation was analyzed by ligation-mediated PCR as described previously (Ishihara et al., 2004).

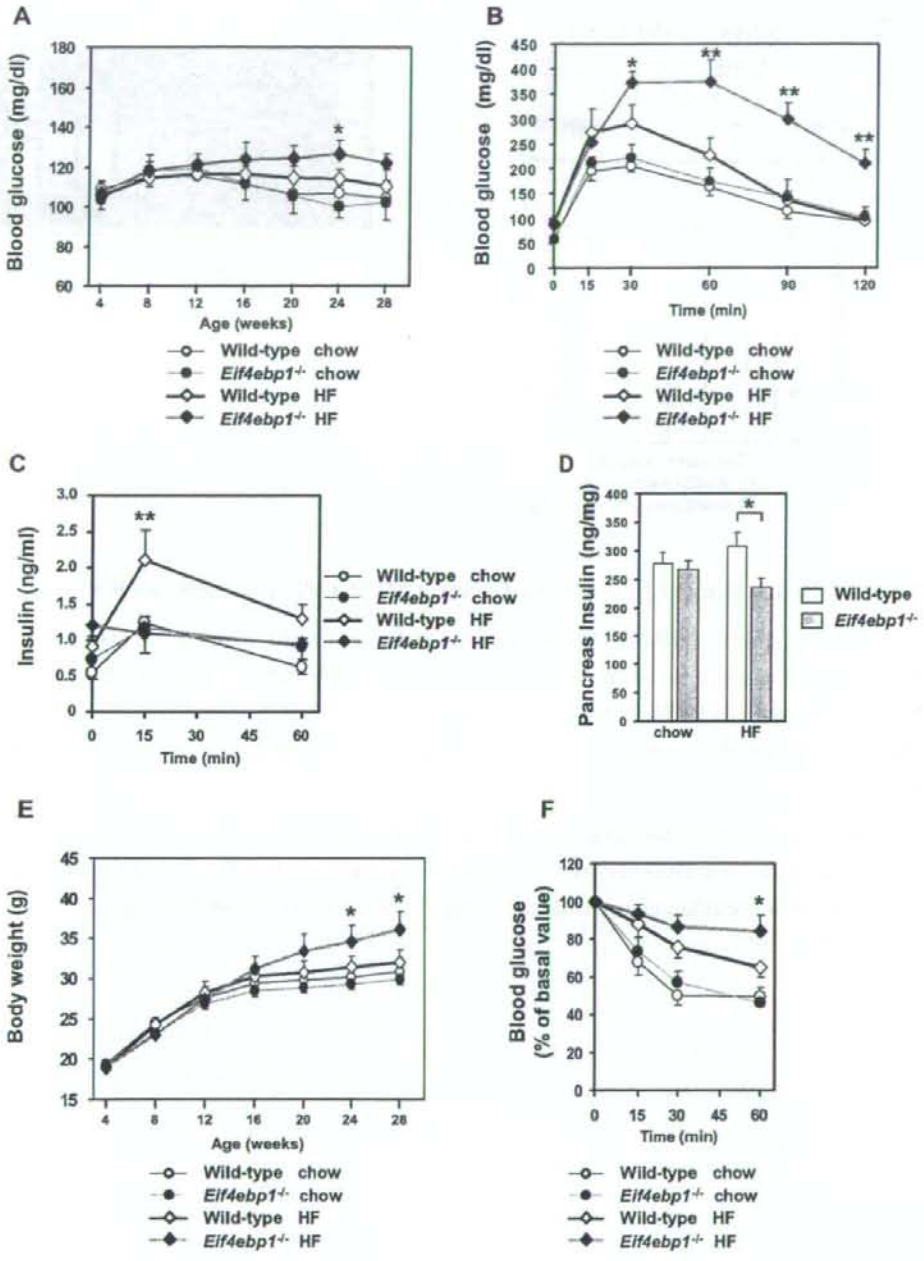
A
Blood glucose (mg/dl)
Age (weeks)
Wild-type chow
Eif4ebp1-/- chow
Wild-type HF
Eif4ebp1-/- HF
B
Blood glucose (mg/dl)
Time (min)
C
Insulin (ng/ml)
Time (min)
D
Pancreas Insulin (ng/mg)
chow
HF
Wild-type
Eif4ebp1-/-
E
Body weight (g)
Age (weeks)
F
Blood glucose (% of basal value)
Time (min)

Figure S4. Body Weight and Glucose Homeostasis in Wild-Type and *Eif4ebp*$^{-/-}$ Mice Fed Standard Chow or a High-Fat Diet

(A) Fed blood glucose levels of wild-type and *Eif4ebp*$^{-/-}$ mice on standard chow or a high-fat diet (HFD; Research Diets D12451).

(B) Blood glucose levels during intraperitoneal glucose tolerance tests (2 g glucose per kg of body weight) in wild-type and *Eif4ebp*$^{-/-}$ mice fed chow or a HFD at 24 weeks of age.

(C) Plasma insulin levels during intraperitoneal glucose tolerance tests (2 g glucose per kg of body weight) in wild-type and *Eif4ebp*$^{-/-}$ mice fed chow or a HFD at 26 weeks of age.

(D) Pancreatic insulin contents of wild-type and *Eif4ebp*$^{-/-}$ mice fed chow or a HFD at 28 weeks of age.

(E) Growth curves of wild-type and *Eif4ebp*$^{-/-}$ mice fed chow or a HFD.

(F) Insulin tolerance tests in wild-type and *Eif4ebp*$^{-/-}$ mice fed chow or a HFD at 25 weeks of age. After a 6 hr fast, mice were given an intraperitoneal injection of insulin (0.75 μU/g body weight). Blood glucose levels at time zero were 69 ± 5 (chow-fed wild-type), 84 ± 11 (chow-fed *Eif4ebp1*$^{-/-}$), 79 ± 5 (HFD-fed wild-type) and 107 ± 6 mg/dl (HFD-fed *Eif4ebp1*$^{-/-}$).

*$p < 0.05$ and **$p < 0.01$, between HFD-fed *Eif4ebp*$^{-/-}$ and HFD-fed wild-type mice. n = 4-6.

Error bars show SEM.

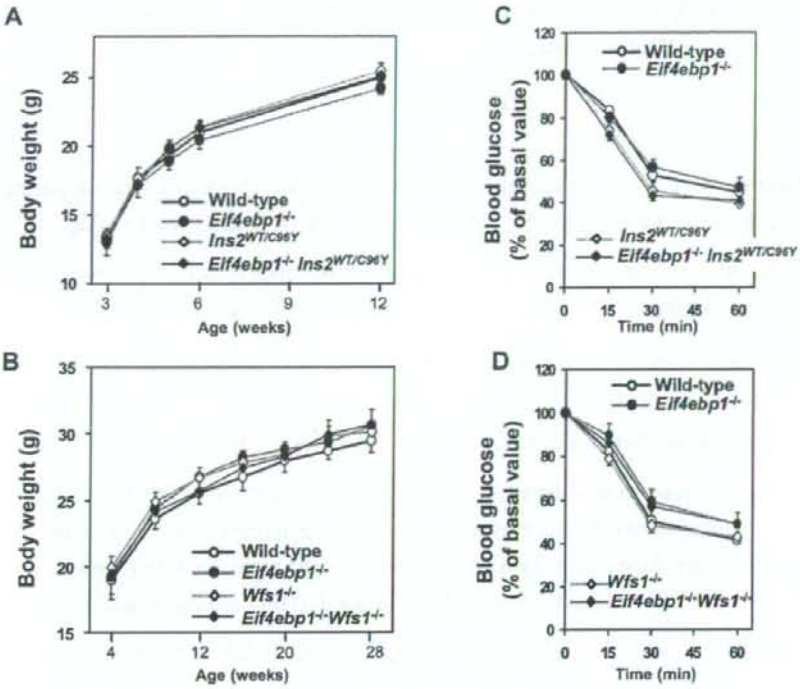

Figure S5. Characterization of 4E-BP1-Deficient *Ins2*$^{WT/C96Y}$ and *Wfs1*$^{-/-}$ Mice

(A) Growth curves of wild-type, *Eif4ebp*$^{-/-}$, *Ins2*$^{WT/C96Y}$ and *Eif4ebp1*$^{-/-}$*Ins2*$^{WT/C96Y}$ mice. n = 5-11.

(B) Growth curves of wild-type, *Eif4ebp1*$^{-/-}$, *Wfs1*$^{-/-}$ and *Eif4ebp1*$^{-/-}$*Wfs1*$^{-/-}$ mice. n = 8-15.

(C) Intraperitoneal insulin tolerance tests in wild-type, *Eif4ebp1*$^{-/-}$, *Ins2*$^{WT/C96Y}$ and *Eif4ebp1*$^{-/-}$*Ins2*$^{WT/C96Y}$ mice at 5 weeks of age. After a 6 hr fast, mice were given an intraperitoneal injection of insulin (0.75 μU/g body weight). Blood glucose levels at time zero were 77 ± 6 (wild-type), 72 ± 5 (*Eif4ebp1*$^{-/-}$), 216 ± 19 (*Ins2*$^{WT/C96Y}$) and 271 ± 23 mg/dl (*Eif4ebp1*$^{-/-}$*Ins2*$^{WT/C96Y}$). n = 5-8. Insulin sensitivities did not differ among the four groups.

(D) Insulin tolerance tests in wild-type, *Eif4ebp1*$^{-/-}$, *Wfs1*$^{-/-}$ and *Eif4ebp1*$^{-/-}$*Wfs1*$^{-/-}$ mice at 24 weeks of age. After a 6 hr fast (time zero), blood glucose was reduced to similar levels in all four groups; blood glucose levels at time zero were 79 ± 6 (wild-type), 73 ± 5 (*Eif4ebp1*$^{-/-}$), 80 ± 7 (*Wfs1*$^{-/-}$) and 77 ± 9 mg/dl (*Eif4ebp1*$^{-/-}$*Wfs1*$^{-/-}$), n = 7-9. Insulin sensitivities did not differ among the four groups ($p > 0.094$).

Error bars show SEM.

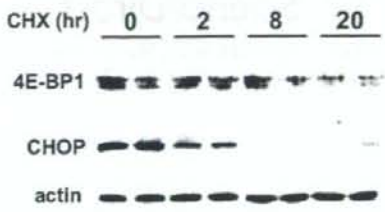

Figure S6. 4E-BP1 Protein Is Stable within Cells

MIN6 cells were incubated with thapsigargin (0.5 μM) for 24 hr, washed with PBS and treated with cycloheximide (CHX, 50 μM) for the indicated period. Cell lysates were subjected to immunoblotting with an anti-4E-BP1 antibody. Immunoblotting results for CHOP are also presented for comparison. The data are representative of three independent experiments.

Supplemental References

Lee, A.-H., Iwakoshi, N.N., and Glimcher, L.H. (2003). XBP-1 regulates a subset of endoplasmic reticulum resident chaperone genes in the unfolded protein response. Mol. Cell. Biol. 2003. *23*, 7448-7459.

Yoshida, H., Okada, T., Haze, K., Yanagi, H., Yura, T., Negishi, M., and Mori, K. (2000). ATF6 activated by proteolysis binds in the presence of NF-Y (CBF) directly to the cis-acting element responsible for the mammalian unfolded protein response. Mol. Cell. Biol. *20*, 6755-6767.

Available online at www.sciencedirect.com
ScienceDirect
Comparative Immunology, Microbiology & Infectious Diseases 31 (2008) 435–448
ELSEVIER
COMPARATIVE IMMUNOLOGY MICROBIOLOGY & INFECTIOUS DISEASES
www.elsevier.com/locate/cimid

Comparative aspects on the role of polypyrimidine tract-binding protein in internal initiation of hepatitis C virus and picornavirus RNAs

T. Nishimura[a,e], M. Saito[a], T. Takano[a,b,c], A. Nomoto[d], M. Kohara[b], K. Tsukiyama-Kohara[a,b,c,*]

[a]*Department of Experimental Phylaxiology, Faculty of Medical and Pharmaceutical Sciences, Kumamoto University 1-1-1, Honjo, Kumamoto 860-8556, Japan*
[b]*Department of Microbiology and Cell Biology, The Tokyo Metropolitan Institute of Medical Science, Tokyo 113-8613, Japan*
[c]*Laboratory Animal Research Center, Institute of Medical Science, The University of Tokyo, Tokyo 108-8639, Japan*
[d]*Graduate School of Medicine, The University of Tokyo, Tokyo 113-0033, Japan*
[e]*The Chemo-Sero-Therapeutic Research Institute, Tokyo 869-1298, Japan*

Accepted 6 July 2007

Abstract

We compared the effects of polypyrimidine tract-binding protein (PTB) on hepatitis C virus (HCV genotype IIa), encephalomyocarditis virus (EMCV) and poliovirus internal ribosome entry site (IRES) activities *in vitro*. It bound strongly to EMCV IRES, but weakly to PV and HCV RNAs. PV IRES showed the strongest dependency to PTB and it showed less than one-tenth of IRES activity after the immuno-depletion of PTB from HeLa S10 lysate with pre-coated anti-PTB IgG beads, comparing to the normal IgG beads-treated S10 lysate. EMCV IRES activity was approximately 40% of that of normal control after PTB depletion.

*Corresponding author. Department of Experimental Phylaxiology, Faculty of Medical and Pharmaceutical Sciences, Kumamoto University 1-1-1, Honjo, Kumamoto 860-8556, Japan. Tel./fax: +81 96 373 5560.
E-mail address: kkohara@kumamoto-u.ac.jp (K. Tsukiyama-Kohara).

0147-9571/$ - see front matter
doi:10.1016/j.cimid.2007.07.002

Especially, HCV IRES activity was approximately 95%, and most weekly affected by the depletion of PTB. Repletion of PTB to depleted S10 lysate restored activities of PV and EMCV IRESs. The data suggest that PTB plays an important role in picornaviral IRESs, but not in HCV IRES.

Keywords: PTB; HCV; IRES; EMCV; PV; HeLa

Résumé

Dans notre étude, nous avons comparé les effet de la 'polypyrimidine track-binding' (PTB) virus de l'hépatite C (génotype IIa) et l'activité du virus encéphalomyodardite (EMCV) et de l'IRES du poliovirus *in vitro*. La PTB se fixe de manière résistante à l'IRES de l'EMCV mais de manière fragile à l'ARN du PV et du VHC. L'IRES du PV montre la dépendance la plus forte à la PTB et il montre une activité d'IRES de moins de un dixième après immuno-déplétion de la PTB du lysat HeLa10 par des billes d'IgG anti-PTB prêtes à l'emploi, par rapport au HeLa10 traité par des billes d'IgG normales. L'activité de l'IRES de l'EMCV était approximativement égale à 40% de celle sous contrôle normal après déplétion de la PTB. L'activité de l'IRES du VHC était approximativement égale à 95% et la moins sensible à la déplétion de la PTB. La réplétion de la PTB au lysat S10 appauvri rétablit les activités des IRES du PV et de l'EMCV. Les données suggèrent que la PTB joue un rôle important dans les IRES picornaviraux mais pas dans les IRES du VHC. De plus,

Mots clés: PTB; VHC; PTB; IRES; PV; HeLa

1. Introduction

Hepatitis C virus (HCV) possesses a single-stranded RNA (approximately 9610 nucleotides), and classified into the family *Flaviviridae* [1–4]. HCV is a major causative agent of non-A non-B hepatitis, and likely progresses into the chronic hepatitis, cirrhosis and hepatocellular carcinoma.

The 5′ untranslated region (5′UTR) of HCV RNA genome is 341 nucleotides and an internal ribosome entry site (IRES) has been proven to exist in this region [5]. Activities of IRESs of HCV were different from each genotype, and genotype IIa showed almost two-fold higher IRES activity than genotype Ib [6,7].

The IRESs have been discovered in the *Picornavirus* genomes and have a complex RNA secondary structure [5,8]. The importance of secondary structure to IRES function is understood by studies that sequence substitutions within the IRES are accompanied by compensatory mutations that act to maintain the RNA secondary structure. The 40S ribosome subunit is recruited within these IRES without binding to the m^7G cap and eIF4E [9,10]. IRESs can be classified into at least 3 groups, according to their features. IRESs derived from entero- and rhinoviruses are classified into type 1(poliovirus), and oligopyrimidine tract is located in 50–100 nucleotides past the 3′ end of the IRES [11,12]. The oligopyrimidine tract

immediately follows the 3′ end of type 2 (cardio- and aphthoviruses) IRES. Encephalomyocarditis virus (EMCV) and foot and mouse disease virus possess type 2 IRESs and utilyzes eIF4G and 4B [13,14]. The HCV and classical swine fever virus (CSFV) possess type 3 IRESs which interact directly to 40S ribosome subunit and eIF3 [15]. In addition to the requirement for eIF in each IRESs, the existence of internal initiation trans-acting factors (ITAFs) has been reported [16,17]. One of ITAFs binds to picornavirus and HCV IRES commonly is polypyrimidine tract-binding protein (PTB) [11,18–20]. PTB may work in each IRESs, however, its exact role in internal initiation has been still unclear at present. In the present study, requirement of PTB in poliovirus, EMCV and HCV IRESs has been characterized, and compared in *in vitro* translation system by depletion and complementation of PTB.

2. Materials and methods

2.1. Isolation of cDNA clones and construction of expression vectors

HCV cDNA that corresponds to nucleotide positions 1-418 (GenBank) was isolated by PCR from plasma of HCV type IIa infected patients [5], using a sense primer, 5′-GATCTAGAGCCCGCCCCCTGATGGGGGCGA-3′, and antisense primer 5′-TGTCCTGCAGTTCAAGGGCCC-3′. The amplified cDNA was digested with XbaI and AatII, and replaced with an XbaI and AatII fragment (5′UTR) of pkIV [5]. A whole cDNA which was excised by XbaI-HindIII was filled up with Klenow fragment (Takara) and cloned into StuI site of pNar3 [5], and the resulting plasmid was designated as pNII5′.

Poliovirus cDNA expression vector T7M2, CAT gene with 5′UTR of EMCV (pBSECAT) and T7CAT were constructed, as described previously [19,21].

PTB cDNA that encodes whole coding region (amino acids no. 1-531) [22] or C terminal half (amino acids no. 291-531) of PTB was synthesized by RT-PCR, and cloned into the downstream of glutathione S transferase (GST) protein in frame in pGEX-KG vector, and was designated as pGST-PTB.

2.2. Expression of PTB and production of specific antibodies

The pGST-PTB was transformed in *Esherichia coli* strain SCS-1 and induced expression with 1 mM IPTG induction. *E. coli* culture (40 ml) was peletted by centrifuge and lyzed with lysozyme (1 mg/ml) and sonicated with 1% TritonX100 and 10 mM DTT. The supernatant was reacted to Glutathione Sepharose 4B (Amersham Bioscience), cleaved by thrombin (SIGMA) and purified with ploy U Sepharose 4B (Amersham Bioscience), as described previously [22]. Rabbits or guinea pigs immunized were over four times intradermal and subcutaneously or intraperitonealy with purified recombinant whole or C-terminal half of PTB (200 μg). These hyperimmune sera were purified by the protein G Sepharose 4B (Amersham Bioscience). The anti PTB rabbit IgG was further purified by the affinity

column of PTB cross-linking Formyl Cellulofine (Seikagaku Kogyo Co.), as described by manufacturer's instruction manual.

2.3. UV cross-linking assays and immunoprecipitation

RNA probes corresponding to nucleotide(nt.) 1-341 of the HCV 5′UTR, nt. 260-833 of the EMCV 5′UTR and nt. 1-747 of the PV 5′UTR were generated by the digestion of pNII5′ with BspHI, pBSECAT with BalI and pM1(T7) with HgiAI, respectively, and transcribed by using Megascript™ T7 RNA polymerase kit (Ambion) with [α-^{32}P]UTP (NEN). Labelled RNA probes were purified by the Nuc Trap™ push columns (Stratagene). Probes ($1-5 \times 10^6$ cpm) were incubated with or without competitor RNA in HeLa S10 lysate (10 μg) at 30 °C for 20 min and irradiated on ice for 20 min in a UV Stratalinker (Stratagene). Unbound RNAs were digested with 10 μg of RNase A (Sigma), 200 units of RNase T1 (Gibco BRL) and 1 unit of phosphodiesterase I (Amersham Bioscience). Samples were analyzed by SDS-PAGE and dried gel was exposed to imaging plate (Fuji) or X-ray film (Kodak). Radioactivity was measured by the Bio-image analyzer BAS 2000 (Fuji).

HeLa S10 or recombinant PTB which was UV cross-linked to labeled HCV RNA was solubilyzed by single lysis buffer containing 1% NP40, reacted with affinity-purified anti-PTB Ig (4 μg) and precipitated by affigel protein A (Bio Rad) beads. Precipitated protein was further characterized by SDS-PAGE.

2.4. Immuno-depletion test

Affigel protein A (Bio Rad) 50 μl was pretreated with HeLa S10 100 μl at 37 °C for 1 h. The affinity purified anti-PTB Rabbit IgG (500 μg) was added, and rotated at room temperature for 3 h. These IgG beads were coated by 10% FCS-0.1 M phosphate buffer (pH 8.0) at 37 °C for 1 h, washed with S10 dialysis buffer (10 mM Hepes-KOH pH7.5, 90 mM KOAc, 1.5 mM $Mg(OAc)_2$), and reacted to HeLa S10 lysate (150 μl) at 4 °C overnight. The supernatants of each reaction were utilized for *in vitro* translation.

2.5. Competitive ELISA

Serocluster 'U' vinyl plate with 96 wells (Costar) was coated with affinity purified rabbit anti-PTB-C term IgG (2.5 μg/ml) at 4 °C overnight. After blocking with 1% casein PBS (−) at 25 °C for 2 h, non-treated or immunodepleted HeLa S10 lysate were added to each well, and incubate at 25 °C for 2 h. Purified recombinant PTB was used for standard and non-treated or immunodepleted HeLa S10 lysates were added to each well, and incubate at 25 °C for 2 h. Then anti-PTB guinea pig IgG (1 μg/ml) was reacted at 37 °C for 1 h, and finally anti-guineapig -IgG HRP (Dako 1:2000) was reacted at 37 °C for 1 h. *Ortho*-phenylene diamine was added to each well as substrate, and the absorbance was measured by microplate reader Model 450 (Bio Rad).

2.6. In vitro transcription and translation

Plasmids were linearized by digestion with XmnI (pNII5′), HpaI (pBSECAT) and NheI (p(M1)T7) and transcribed into RNA by Megascript™ T7 RNA polymerase kit (Ambion). RNAs were treated with DNase I, precipitated with LiCl, and quantitated by the Spectrophotometer DU64 (Beckman).

Synthetic RNAs (pNII5′ RNA; 1.0 pmol, pBSECAT; 1.8 pmol, p(M1)T7; 0.36 pmol and they were optimized for the linear phase in translation activity) were translated in HeLa S10 lysates at 37 °C for 30 min with [^{35}S]-Methionine (ICN), as described previously[5] . Translation products were analyzed using 7.5–15% gradient SDS-PAGE.

2.7. Restoration assay

Purified recombinant PTB, bovine serum albumin and ribosome salt wash (RSW) were dialyzed to S10 dialysis buffer, and added to PTB depleted or non-treated HeLa S10. RSW (total 6.7 ml) was prepared from 6.1 l of HeLa S10, as described previously [5] (kindly supplied by Dr. H. Toyoda).

3. Results

3.1. Fifty-seven and 60 kDa doublet protein bound HCV, EMCV and PV RNA

HeLa cytoplasmic proteins that were detected by UV cross-linking to ^{32}P-UTP labeled RNA derived from the HCV, EMCV, and PV 5′UTR were compared (Fig. 1). Total counts of binding proteins in HCV RNA was five times lower than those of EMCV RNA, and three times lower than those of PV-RNA (PSL; HCV 21536.9, EMCV 105622.8, PV 59307.9). Among these cytoplasmic proteins, 57 and 60 kDa doublet bands on HCV RNA,EMCV RNA and PV RNA have been identified to be PTB (Fig. 1, indicated by asterisk). According to band intensities of the 57 and 60 kDa proteins, PTB bound to EMCV IRES most abundantly, and more diminished amount of PTB bound to PV and HCV IRESs (Fig. 1).

3.2. Identification of P57/60 kDa doublet protein on HCV-RNA as PTB

HCV-IRES-binding proteins with molecular weight of 57/60 kDa were further characterized. The recombinant PTB protein was expressed in *E. coli.* in the presence of IPTG, purified by glutathione sepharose and polyU sepharose column (Fig. 2A), and reacted with affinity purified anti-PTB IgG (Fig. 2B), as described in Section 2. Labeled HCV RNA 5′UTR was cross-linked to HeLa S10 lysate, and immunoprecipitated by affinity purified anti-PTB IgG (Fig. 3). The 57 and 60 kDa doublet bands were specifically reacted to the anti-PTB IgG (Fig. 3, lane HeLa). The recombinant PTB protein was cross-linked with HCV RNA 5′UTR and precipitated with anti-PTB IgG (Fig. 3, lane PTB). These results strongly indicate that PTB

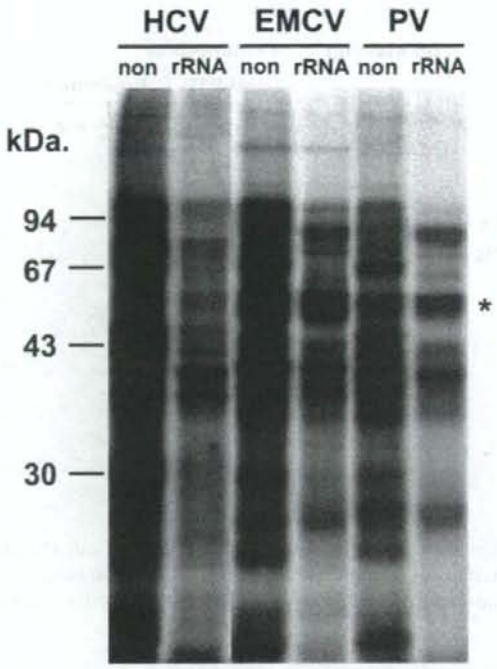

Fig. 1. UV-cross-linking analysis of binding factors to HCV, EMCV and PV-IRES RNAs. Each reaction without competitor indicates "non", and with competitor rRNA indicates rRNA on the top of the lanes. Asterisk indicates the position of PTB proteins. An asterisk indicates PTB binding.

specifically bound to HCV RNA 5′UTR, and observed as doublet protein with molecular weight of 57 and 60 kDa.

3.3. Depletion of PTB in HeLa S10 lysate

Previous results indicated the possibility that other factors than canonical eukaryotic translation initiation factors (eIFs) are working in cap independent translation. PTB is one of the candidates and when the PTB might be commonly used in several kinds of IRESs, it might play the central role in internal initiation. To compare the significance of PTB in translation initiation in HCV and other Picorna virus IRESs, PTB in HeLa S10 lysate was depleted by affinity purified anti-PTB IgG. For the depletion of PTB, pre-coating of Affi-gel protein A beads was necessary to block the non-specific adsorption, as described in Section 2. Pre-coated beads were reacted with anti-PTB IgG. From the preliminary experiments, more than 100 times higher molar ratio of anti-PTB IgG to PTB in S10 lysates was required for the over 90% depletion, as described in Materials and methods. We performed the PTB depletion, and 94.5% of PTB was depleted by anti-PTB IgG and 26.3% of PTB was depleted by pre-immune IgG (Fig. 4). We further examined the effect of PTB

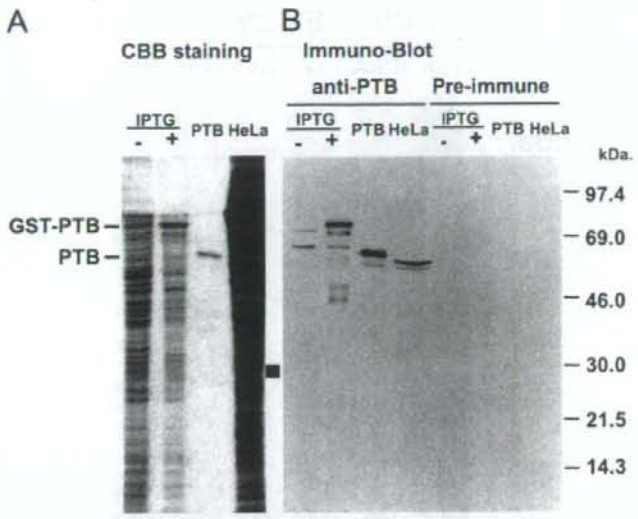

Fig. 2. Expression of recombinant PTB protein fused with GST in *E. coli*: (A) Expression of PTB protein was induced by IPTG, purified by glutathione sepharose column and stained with CBB. (B) Expressed recombinant PTB was transferred to membrane and reacted with specific antibody by WB.

depletion to the binding of cellular factors to three IRESs (Fig. 5). In PTB depleted lysates, binding of 57 and 60 kDa doublet protein was decreased, especially in PV-RNA. However, binding of other factors was not influenced significantly, other than 28 kDa protein (Fig. 5, indicated by an arrow).

3.4. *Effect of PTB depletion in translation*

Influence of PTB depletion was examined in HCV, EMCV and PV-RNA (Fig. 6A, Table 1). The reaction curves of each RNA were different from each other (data not shown), and the optimum quantity of each RNA used in this study was different from each other (Table 1). From the comparison of translation activity in PTB depleted S10 lysates, translation of PV-RNA was significantly decreased in 4 and 8 μl lysates (22–4.5%, 15–0.9%, Table 1, Fig. 6A). Translation of EMCV-IRES was significantly decreased after PTB depletion (53–44% (4 μl), 28–11% (8 μl)), but this suppression was not as much as PV-IRES. Activity of HCV-IRES was almost similar between pre-immune IgG-treated and anti-PTB IgG-treated S10 lysates. Because the optimal RNA quantities for translation are different in each IRESs, therefore, we calculated the ratio of PTB quantity per template RNA molecules (PTB/RNA) (ng/pmol; Table 1). In PV-IRES, translation activity was significantly reduced after depletion (4.5%, 0.9%) and the PTB/RNA ratio was 1.4 and 0.56. EMCV-IRES and HCV-IRES activity. Influence of PTB depletion to HCV-IRES activity was much lower than those of PV and EMCV.

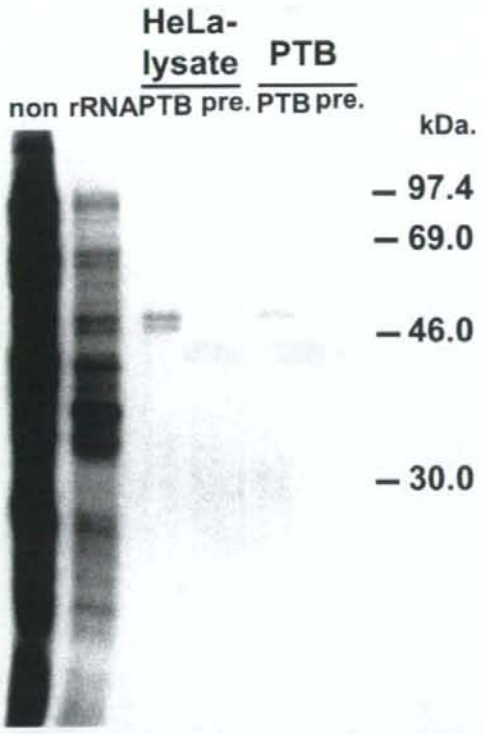

Fig. 3. HCV-IRES cross-linked S10 and PTB was immuno-precipitated by purified anti PTB antibody and pre-immune antibody. The 57 and 60 kDa doublet bands were specifically reacted to the anti-PTB IgG (lane HeLa). The recombinant PTB protein was cross-linked with HCV RNA 5′UTR and precipitated with anti-PTB IgG (lane PTB). Pre-immune antibody did not reacted to both Hela S10 and PTB.

The IRES activity of EMCV and PV-RNA was decreased by treatment of pre-immune IgG, however, treatment of pre-immune IgG did not influence significantly to the IRES activity of HCV-RNA.

3.5. Restoration of PTB to depleted S10

To clarify the effect of immuno-depletion was mainly caused by the decreased quantity of PTB, the purified recombinant PTB or RSW was added to depleted S10 (Fig. 6B). The IRES activity of PV-RNA in depleted S10 lysate (6 μl) was increased by the addition of PTB in dose-dependent manner. The EMCV-IRES activity was recovered even in the presence of 1 μg of PTB in depleted S10 lysate (4.0 μl). When too much quantity of PTB was added to the S10, translation activity of PV, EMCV and HCV decreased (over 10 times of PTB in PV, over 300 times in EMCV and over 500 times in HCV RNA, data not shown).

Translation activity of PV and EMCV-RNA became higher after the addition of RSW to anti-PTB IgG depleted S10 (150% and117%, respectively) (date not